Chinese Journal of Aeronautics 25 (2012) 681-690

Contents lists available at ScienceDirect

Chinese Journal of Aeronautics

journal homepage: www.elsevier.com/locate/cja

Airworthiness Compliance Verification Method Based on Simulation of Complex System

XU Haojun*, LIU Dongliang, XUE Yuan, ZHOU Li, MIN Guilong

Department of Aircraft and Aeroengine, The Engineering Institute, Air Force Engineering University, Xi'an 710038, China

Received 28 September 2011; revised 24 December 2011; accepted 12 January 2012

Abstract

A study is conducted on a new airworthiness compliance verification method based on pilot-aircraft-environment complex system simulation. Verification scenarios are established by "block diagram" method based on airworthiness criteria. A pilot-aircraft-environment complex model is set up and a virtual flight testing method based on connection of MATLAB/Simulink and Flightgear is proposed. Special researches are conducted on the modeling of pilot manipulation stochastic parameters and manipulation in critical situation. Unfavorable flight factors of certain scenario are analyzed, and reliability modeling of important system is researched. A distribution function of small probability event and the theory on risk probability measurement are studied. Nonlinear function is used to depict the relationship between the cumulative probability and the extremum of the critical parameter. A synthetic evaluation model is set up, modified genetic algorithm (MGA) is applied to ascertaining the distribution parameter in the model, and a more reasonable result is obtained. A clause about vehicle control functions (VCFs) verification in MIL-HDBK-516B is selected as an example to validate the practicability of the method.

Keywords: aircraft; airworthiness; certification; pilot model; flight simulation; flight safety

1. Introduction

Airworthiness compliance verification is an essential part for a new aircraft to obtain its airworthiness certificate (AC). Methods of airworthiness compliance verification involve compliance statement, explanatory documents, analysis/calculation, safety assessment, laboratory tests, aircraft ground test, flight testing, aircraft inspection and equipment eligibility inspection. However, to verify the safety performance of the whole aircraft affected by unfavorable factors, the above ten methods are not enough. Those traditional methods, such as laboratory test, aircraft ground test and flight testing have their weaknesses such as high cost, long time for preparation and execution, and difficulties in checking all flight conditions in aircraft operational domain, especially in complex and critical situations [1-2].

The verification method based on complex system simulation has its unique advantages. A) This new airworthiness verification method could be applied to the phase of aircraft design, so that the design process can be optimized, the cost reduced, and schedule shortened. B) Conducting "virtual flight-testing" prior to detailed design can reduce the cost greatly with the total amount of test and certification (T&C) flight hours being reduced. C) A safer and more accurate flight envelope is formed by conducting safety assessment in complex and critical conditions, thus enhancing aircraft airworthiness and safety level [3-4].

Airworthiness verification always refers to risk probability assessment. The occurrence probability of flight accident is very small. Therefore, small risk evaluation method using limited amount of samples obtained from "pilot-aircraft-environment" complex system simulation is a significant problem to be solved [5].

*Corresponding author. Tel.: +86-29-84787637.
E-mail address: xuhaojun@mail.xjtu.edu.cn

Foundation items: National Natural Science Foundation of China (60572172, 61074007)

doi:10.1016/S1000-9361(11)60434-2

2. Modeling of Complex System Based on Verification Scenario

Modeling of "pilot-aircraft-environment" system is the groundwork of system simulation. And the modeling is always based on specific scenario. So the first step of airworthiness verification is the construction of a scenario according to specific airworthiness clause. There are three components in the complex system, including pilot, aircraft and environment.

2.1. *Potential hazard analysis and establishment of scenarios*

Scenarios of flight testing are established according to clauses in airworthiness criteria [6]. In the U.S., Federal Aviation Regulations (FAR) are promulgated by Federal Aviation Administration (FAA). FAR series are the standards for air traffic control, qualification of production license and airworthiness certificate, etc. The U.S. has more comprehensive civil aviation airworthiness criteria, such as FAR 23, 25, 27, 33 which include specific airworthiness standards for various systems of the aircraft. China Civil Aviation Regulations (CCAR) series are formed on the basis of the U.S. civil aviation airworthiness standards. Currently, the U.S. F-22, F-35 and other advanced fighters have brought in airworthiness idea and used MIL-HDBK-516B as the basis for aircraft design.

Accident chain starts from hazard factors. Thus, potential hazard analysis of certain clauses in airworthiness criterion is the basis of the scenarios' establishment. Hazard analysis methods include fault mode and effect analysis (FMEA), event tree analysis (ETA), fault tree analysis (FTA), hazard checklist method, engineering experience method, etc [7].

"Block diagram" is adopted in this paper to establish scenarios. The function of scenario is depicting potential accident chains in a certain airworthiness clause. Its main components include potential hazard factors effecting flight safety, effects of hazard factors on aircraft motion and safety decisive parameters.

An example is introduced to illustrate the process of founding a flight scenario. Clause 6.2.4.2 in vehicle control functions (VCFs) in Chapter 6 of MIL-HDBK-516B is selected. The specification of this clause is "all single point failures are identified with the associated probability of failure(s) and that they demonstrate an acceptable flight safety risk" [8].

Using the "cannikin law", the weakest link of the VCF should be found first. According to the reliability test of a fly-by-wire and the flight record of the exemplified aircraft, n_z (normal overload) sensor and roll rate sensor are the organs that most likely to fail [9]. Thus, there are two potential accident chains caused by two sensors' malfunction. Failures of sensors lead to the malfunction of elevator and aileron. The safety decisive parameters of the two possible accident chains are α (angle of attack (AOA)), n_z or p (roll rate). Flight scenario of this clause is shown in Fig. 1.

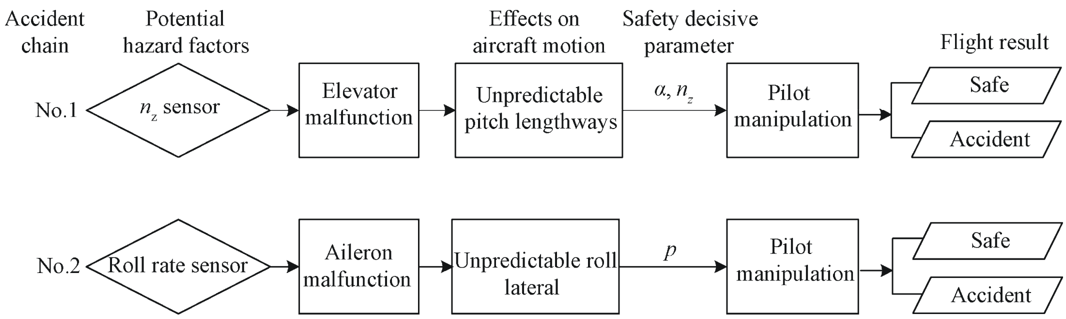

Fig. 1 Flight scenario of Clause 6.2.4.2 in MIL-HDBK-516B.

2.2. *Stochastic pilot model*

1) Stochastic modeling of pilot behavior parameters

Statistical property analysis of pilot behavior parameters show that the static gain of pilot K_p, with minimal constraints, is close to meeting the lognormal distribution law. The lognormal distribution density function of random variable x is [10]

$$f(x)=\frac{1}{x\sigma\sqrt{2\pi}}\exp\left[-\frac{1}{2\sigma^2}(\ln x-\ln\mu)^2\right] \tag{1}$$

where $\ln\mu=\frac{\sum_{i=1}^{N}\ln x_i}{N}$, N is the number of random variable x, $\sigma=\sqrt{\frac{\sum_{i=1}^{N}(\ln x_i)^2-(\sum_{i=1}^{N}\ln x_i)^2 \Big/ N}{N-1}}$.

Histogram is established according to parameter identification of the pilot manipulation. Through comparison, it can be seen that the model based on lognormal distribution law (solid line) is more accurate than the model based on normal distribution law (triangle line), as shown in Fig. 2.

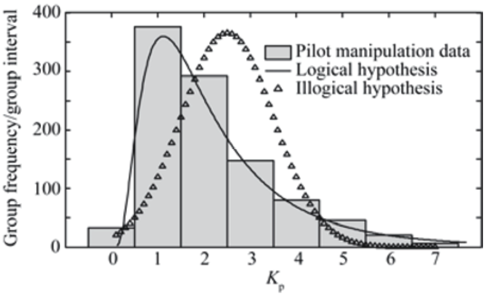

Fig. 2 Lognormal distribution density function and histogram.

(0, 1) uniform distribution is the simplest and most basic distribution law. Any other random variable can be obtained through its transformation. Mathematical methods can be used to obtain random numbers that submit to other distribution from (0, 1) uniform distribution. The following text refers to the deduction of logarithmic normal distribution and truncated normal distribution random numbers' generation method.

According to the lognormal distribution density function, set

$$F_x = \int_0^x \frac{1}{x\sigma\sqrt{2\pi}} \exp\left[-\frac{1}{2\sigma^2}(\ln x - \ln\mu)^2\right] \mathrm{d}x \tag{2}$$

If $\hat{\mu} = \ln\mu$, $\hat{x} = \ln x$, then

$$F_x = \int_{-\infty}^{e^x} \frac{1}{x\sigma\sqrt{2\pi}} \exp\left[-\frac{1}{2\sigma^2}(\hat{x} - \hat{\mu})^2\right] \mathrm{d}\hat{x} \tag{3}$$

$Y = \{y_1, y_2, \cdots, y_n\}$ obeys the $N(\hat{\mu}, \sigma^2)$ distribution; order $z_i = e^{y_i}$, then the random $Z = \{z_1, z_2, \cdots, z_n\}$ obeys lognormal distribution.

Inverse transformation principle is used to generate random numbers subject to the truncated normal distribution. Set that random number m_i obeys (0,1) uniform distribution. If $m_i < 0.5$, then m_i falls into the range of left-censored; if $m_i \geq 0.5$, then m_i falls into the right-censored interval. When it is in the left truncated interval, then

$$m_i = \int_{D_{\min}}^x \frac{1}{c_1\sigma_1\sqrt{2\pi}} \exp\left[-\frac{1}{2\sigma_1^2}(x-\mu_1)^2\right] \mathrm{d}x =$$

$$\int_{-\infty}^x \frac{1}{c_1\sigma_1\sqrt{2\pi}} \exp\left[-\frac{1}{2\sigma_1^2}(x-\mu_1)^2\right] \mathrm{d}x -$$

$$\int_{-\infty}^{D_{\min}} \frac{1}{c_1\sigma_1\sqrt{2\pi}} \exp\left[-\frac{1}{2\sigma_1^2}(x-\mu_1)^2\right] \mathrm{d}x$$

$$c_1 m_i = \int_{-\infty}^x \frac{1}{\sigma_1\sqrt{2\pi}} \exp\left[-\frac{1}{2\sigma_1^2}(x-\mu_1)^2\right] \mathrm{d}x -$$

$$\int_{-\infty}^{D_{\min}} \frac{1}{\sigma_1\sqrt{2\pi}} \exp\left[-\frac{1}{2\sigma_1^2}(x-\mu_1)^2\right] \mathrm{d}x$$

$$c_1 m_i + m_0 = \int_{-\infty}^x \frac{1}{\sigma_1\sqrt{2\pi}} \exp\left[-\frac{1}{2\sigma_1^2}(x-\mu_1)^2\right] \mathrm{d}x \tag{4}$$

where $D_{\min}$ is the minimum value of x, c_1 a positive constant, σ_1 the variance of x, m_0 the cumulative probability $(m_0 = P(X \leq D_{\min}))$.

According to the distribution of $N(\mu, \sigma^2)$, the maximum of random numbers x_i is calculated with the cumulative probability $c_1 m_i + m_0$. Similarly, process m_i which falls into the right-censored interval, and $X = \{x_1, x_2, \cdots, x_n\}$ obeys the truncated normal distribution.

The simulated pilot behavior parameters gained through the above-mentioned mathematical methods have eight groups, as shown in Table 1. In the table, τ is the time delay, T_1 is the lead compensation time constant, T_2 is time delay of transmission and processing of central informationn, T_N is the neuromuscular delay time.

Table 1 Pilot model parameters

Simulation results	K_P	τ	T_1	T_2	T_N
1st	2.020	0.105	0.213	0.274	0.094
2nd	1.627	0.204	0.093	0.331	0.312
3rd	2.267	0.076	0.226	0.163	0.168
4th	1.239	0.264	0.112	0.236	0.041
5th	2.117	0.210	0.312	0.121	0.177
6th	1.319	0.335	0.505	0.093	0.085
7th	5.587	0.108	0.204	0.618	0.055
8th	1.205	0.172	0.143	0.259	0.108
Mean value	2.173	0.184	0.226	0.262	0.130
Variance	2.075	0.008	0.018	0.024	0.008

The calculated mean and variance are close to the identification of the true results. Taking the first simulation for example, the results of pilot model simulation match the real practice, which is shown in Fig. 3. In the figure, T is the simulation time.

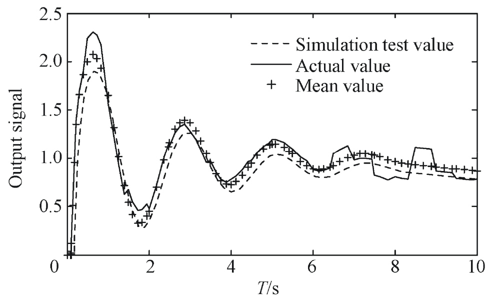

Fig. 3 Output signal of pilot behavior stochastic model.

2) Pilot manipulation model in critical situation

The research is focused on pilot manipulation modeling after a severe failure of certain key system. Pilot feels drastic change of acceleration caused by the failure, and has the response to counteract this change by manipulation. The pilot's control strategy can be understood as eliminating the sudden change of flight status, reducing adverse consequences as caused by non-human factors.

The established pilot model is shown in Fig. 4. In the figure, Y (f_0, x_0, v_0, t) is the function, f_0 is rod rorce, x_0 is rod displacement, v_0 is speed of pilot manipulate the rod, t is time of pilot manipulate the rod.

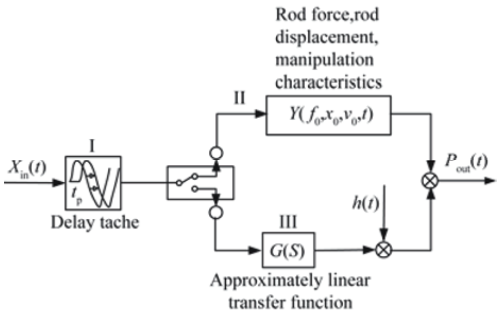

Fig. 4 Pilot control model for special circumstances.

Assuming that the initial pilot handling characteristic involved in closed-loop control is $Y(t)$, the effective time is ΔT, the time that unit II converts to unit III is $t = t_p + \Delta T$, where t_p is the delay time of pilot manipulation, and according to the conversions between units at different time instants, the model's input-output relationship can be described as

$$P_{out}(t) = \begin{cases} 0 & t \le t_p \\ Y(t)\,X_{in}(t) & t_p < t \le t_p + \Delta T \\ G(t)\,X_{in}(t) + h(t) & \text{Safe}, t \ge t_p + \Delta T \\ 0 & \text{Accident}, t \ge t_p + \Delta T \end{cases} \quad (5)$$

where P_{out} is the final output of pilot, $X_{in}(t)$ the input offset signal, $G(t)$ the pilot quasilinear function when the changes of flight parameters are stable, $h(t)$ pilot noise function.

The most important parameter of the model is the delay time of pilot manipulation t_p. In this paper, the probability distribution method is used to establish the mathematical model of t_p.

Pilot average response delay time t_b calculated by simulation is 1.209. Formula $\ln t_B = \ln \frac{t_b}{\sqrt{k^2+1}}$ is applied [10] to gaining the mathematical expectation of the delay time: $\ln t_B = -0.043\,8$. A constant to describe the differences of pilot manipulation in tilt channel is $k = 0.5$, and the variance of latency is calculated to be $D = 2\ln\sqrt{k^2+1} = 0.223\,1$. The pilot manipulation delay time subjects to lognormal distribution t_p obeys $\mathrm{LN}(-0.043\,8, -0.223\,1)$.

The simulation result of pilot delay time stochastic model using Monte Carlo method is shown in Fig. 5.

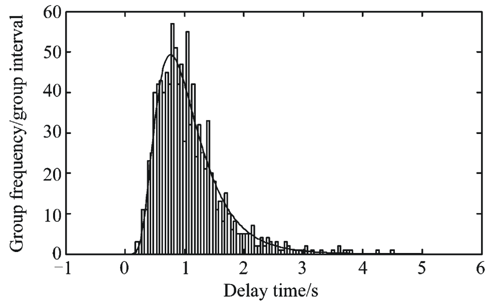

Fig. 5 Pilot delay time stochastic model.

2.3. *Aircraft model and external environment modeling*

Flight risk is always related to scenario in critical state. Due to coupling and non-linear characteristics of parameter changes, the non-linear six-degree-of-freedom mathematical model of aircraft flight dynamics is adopted. These equations are a set of high-rank non-linear coupling differential coefficient equations, from which dynamic characteristics of an aircraft is obtained. Generally, appropriate equation simplification can be made according to specific problem. In the study of rolling characteristics, changes of velocity can be neglected, so equations can be changed into five-degree-of-freedom differential coefficient equations.

Aircraft fly-by-wire control system is usually constructed on the basis of Simulink. For a specific aircraft, the model of airframe and control system is fixed.

The key point of environment research is adverse operational situation, involving some events and phenomena in atmospheric environment or in air corridor, which could threaten flight safety. Such events and phenomena include adverse weather condition (wind shear, turbulence, heavy rain, icing, thunderstorm, atmosphere discharge), flying birds and possible objects that may cause collision, wake vortex left by aircraft, wet runway, etc. The corresponding simulation model can be set up according to specific situation [11], and the related impact on aircraft movement is involved in the equations.

3. Potential Risk Analysis and Reliability Modeling of Scenarios

3.1. *Analysis of potential risk*

The risks of flight testing come mainly from the following aspects: risks from new products, new systems and new component parts, risks from critical flying conditions, risks from technologies in new explored areas, and risks caused by human factors and adverse environment.

Changes that take place from hazard to accident is an evolution process of the system status. The transition process from safe to unsafe state can be depicted as an accident chain (see Fig. 6).

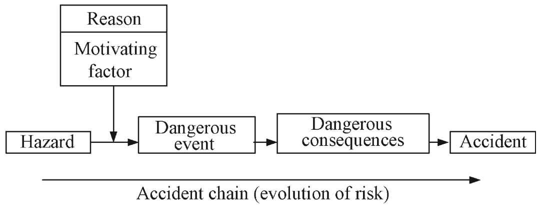

Fig. 6 Block diagram of risk evolution.

Risk analysis methods include FMEA, ETA, FTA, hazard checklists law, and engineering experience method, etc [7]. Based on the theory of accident chain and the ideas of FMEA, mathematical models of representative failure mode are established as follows.

3.2. *Failure mode modeling and effects analysis*

The performance type of the failure is called failure mode, which describes the basic characteristics of product failure. Research of failure model involves three aspects, failure mode, failure impact on flight safety, and failure probability. The failure mode concept provides clues and evidence for fault identification and comprehensive failure analysis. Typical failure modes are shown in Table 2.

Table 2 Typical failure modes

Serial number	Failure mode	Serial number	Failure mode
1	Structural failure (broken)	10	External leak
2	Tied knot, or stuck on	11	Beyond tolerance (maximum)
3	Vibration	12	Beyond tolerance (minimum)
4	Failure to keep the normal position	13	Run accident
5	Failure to open	14	Intermittent work
6	Failure to close	15	Shift work
7	Open error	16	Error indication
8	Close error	17	Poor circulation
9	Internal leak	18	Incorrect action

Modeling of system's weak links is an important foundation for flight safety quantitative assessment. In this paper, research is conducted on the modeling of aircraft failures in key systems, and fly-by-wire system is taken as an example.

Fly-by-wire system failures occur generally in two aspects, including sensor failure and actuator failure. The mathematical models of sensor failure modes are established as follows:

$y_{i\text{out}}$ represents the actual output of No. i sensor, and $y_{i\text{in}}$ represents the normal input of No. i sensor.

1) Sensor stuck model

The failure model of No. i sensor is

$$y_{i\text{out}}(t) = a_i \tag{6}$$

where a_i is a constant, $i = 1, 2, \cdots, m$.

2) Failure model of sensor constant gain changes

The failure model of No. i sensor is

$$y_{i\text{out}}(t) = \beta_i y_{i\text{in}}(t) \tag{7}$$

where β_i is the constant changes in the proportion of the gain coefficient, $i = 1, 2, \cdots, m$.

3) Constant bias sensor failure fault model

The failure model of No. i sensor is

$$y_{i\text{out}}(t) = y_{i\text{in}}(t) + \varDelta_i \tag{8}$$

where $\varDelta_i$ is a constant, $i = 1, 2, \cdots, m$.

4) General sensor fault model

The failure behavior of the above three sensors could result in control function errors, so for the control system type, a sensor fault is usually expressed as

$$\begin{cases} x(t) = \boldsymbol{A}x(t) + \boldsymbol{B}u(t) \\ y(t) = \boldsymbol{C}x(t) + \boldsymbol{Q} f_s(t) \end{cases} \tag{9}$$

where $\boldsymbol{A}$ is the state matrix, $\boldsymbol{B}$ the input matrix, $\boldsymbol{C}$ the output matrix, $\boldsymbol{Q} \in \mathbf{R}^{m\times g}$ the sensor fault distribution matrix, and $f_s(t) \in \mathbf{R}^g$ the function of the failure impact on the system output.

4. Risk Probability Assessment Model

4.1. *Basic model*

S is the cumulative probability series, and $x \in S$. R is the random variable set of extremum sample, and $y \in R$. On the double negative logarithm scaling axis (DNLSA), the coordinate of x is $x'=-\ln(-\ln x)$ [12].

It can be supposed that $x' \in S'$, and S' is the set of cumulated probability series on the DNLSA.

According to the scatter plot, the mapping $g(S'\to R)$ can be ascertained. By statistical analysis on a number of data groups, it can be found that the scatter diagrams are likely to be linear distribution adopting DNLGA. So the mapping can be solved by linear regress as expressed in[13]

$$g(\cdot) = ax'+b \tag{10}$$

where a and b are the coefficients of the equation. So the nonlinear function is

$$f'(x) = a(-\ln(-\ln x)) + b \tag{11}$$

The occurrence probability is

$$P = 1 - f'^{-1}(y_{\text{li}}) \tag{12}$$

where y_{li} is the limit of y.

4.2. *Nonlinear regress model*

In fact, extremum samples are restricted by boundary, and this fact is not considered in the basic model. Thus, a calculation model containing adjusting parameter is set up in this paper by nonlinear regress.

The function $y = \sqrt[c]{-b/\ln x}$ is selected as the match curve. It can be transformed to $\ln x = -b/y^c$.

The assessment model $F(Y) = \mathrm{e}^{-\frac{b}{Y^c}}$ is set up. It can be deduced that $Y = \ln y$, $X = -\ln(-\ln x)$, $k = 1/c$, $b'=k\ln b$. Hence, the linear function is obtained

$$Y = kX + b' \tag{13}$$

The nonlinear regress model is

$$F(Y)=\begin{cases}\mathrm{e}^{-\frac{b}{(L-Y)^c}} & Y\le L\\ 1 & Y>L\end{cases} \tag{14}$$

where L is the boundary value of random extreme samples.

The model can be considered a linear model after logarithm transformation of the cumulative probability and double negative logarithm function transformation of random extremum.

4.3. Synthesis assessment model

The scattered points on transformed coordinates are linear fitting in the nonlinear model, but larger error may be produced. It can be more precise applying cubic polynomial. The synthesis assessment model is set up.

$$\begin{cases}Y'=\ln(L-y)\\ X=-\ln(-\ln x)\\ Y'=C_4X^3+C_3X^2+C_2X+C_1\end{cases} \tag{15}$$

The parameters C_4, C_3, C_2, C_1 of the polynomial can be obtained by least-square method. And the objective function is the error in the transformed coordinates. It will be more reliable that the target function is the error in the original coordinates. The objective function can be expressed as

$$E=\sqrt{\sum_{n=1}^{k}(Y_n^{'}-f(F(Y_n^{'})))^2} \tag{16}$$

The objective function is complex and nonlinear. The adjusting parameter for distribution can be optimized by modified genetic algorithm (MGA) [14]. Genetic algorithm (GA) can search for the optimal solution by random mode and has a better ability as a whole. But the algorithm is weak in local searching, and easy to become premature. Simulated annealing has a stronger capability in local searching. To avoid the disadvantage of GA, a mixed algorithm applying simulated annealing (SA) to GA is adopted, and the flow chart is shown in Fig. 7.

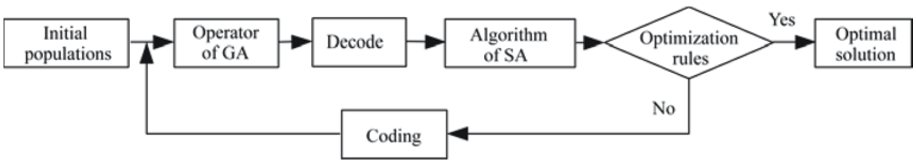

Fig. 7 Flow chart of MGA.

The mode of coding is binary-valued. The fitness is acquired from the transformation of the objective function and adjusted by fitness linear scaling for population diversity. Operation of GA is the adaptive genetic algorithm (AGA) proposed by Srinvivas, which can adaptively choose the probability of crossover and mutation. In order to avoid getting the local optimal solution in early evolution, the elitist selection is adopted [15].

4.4. Calculation case

In certain aircraft flight status, the safety critical parameter is lift coefficient C_L. Twenty extreme samples are obtained by flight data recorder (FDR) and shown in Table 3. The limit value of C_L is x_{li}=1.25, and the parameters cannot reach the boundary value 1.4 [9].

Figure 8 depicts the whole process of GA, and Fig. 9 describes the searching process of SA for one time. It can be found that the calculation on the synthesis assessment model converges by using MGA. The fractional error is in the range of 8, and the detailed calculation results are shown in Table 4. The curve of the approximating function for the optimal solution is shown in Figs. 10-11. Risk probability is 0.040 2.

Table 3 Samples of extremum of critical parameter C_L

Data 1 group	0.688	0.722	0.822	0.902	0.698	0.657	0.753	1.095	0.634	0.648
Data 2 group	0.932	0.720	0.591	0.798	0.929	0.564	0.743	0.753	1.210	0.696

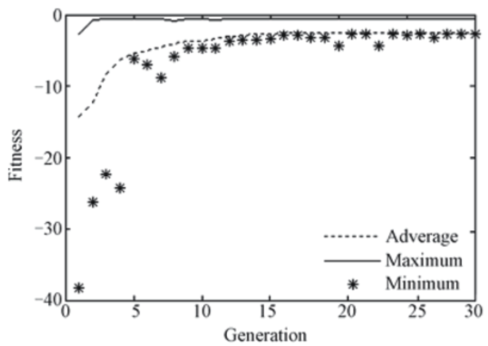

Fig. 8 Process of searching for optimal solution (GA).

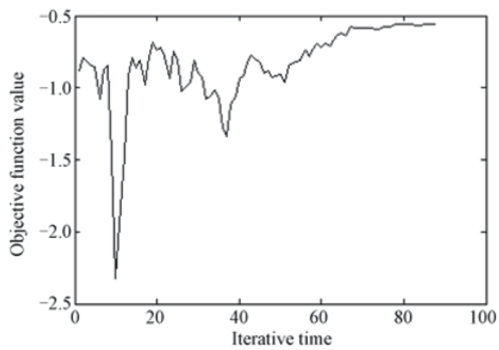

Fig. 9 Process of searching for optimal solution (SA).

Table 4 Calculation results

Arithmetic		Coefficient $C/10^{-2}$				Fractional error/10^{-4}	Probabilistic risk/10^{-2}
		C_1	C_2	C_3	C_4		
GA		−34.95	−14.45	−2.40	−2.45	57.54	3.86
MGA	1	−35.43	−14.04	−1.54	−2.88	55.94	4.02
	2	−35.42	−14.12	−1.52	−2.82	55.99	3.95
	3	−35.19	−14.11	−1.60	−2.76	56.20	3.90
	4	−35.25	−13.82	−1.51	−2.98	55.96	4.21

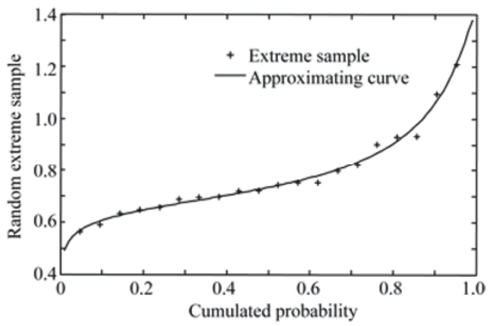

Fig. 10 Curve of the approximating function (linear).

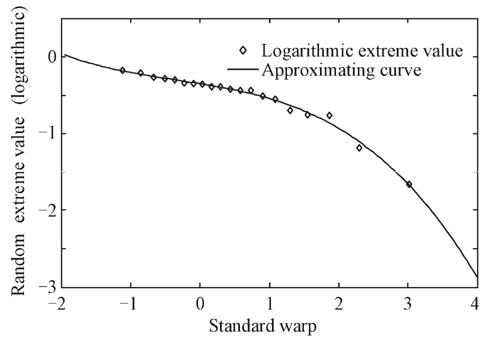

Fig. 11 Curve of the approximating function (DNLSA).

5. Main Idea of the Method

The main idea of the airworthiness compliance verification based on the complex system simulation proposed in this paper can be illustrated in Fig. 12.

The verification process can be divided into six steps:

1) Verification scenario is established according to airworthiness standards and correlative materials.

2) Pilot-aircraft-operational environment model is built based on the scenario established in Step 1.

3) Hazard analysis and reliability modeling are carried out to obtain potential hazards of the system and occurrence rate of hazards.

4) The scenario is simulated in a computer based on the work done in Step 2 and Step 3, which can also be called virtual flight testing.

5) The extreme value of determined parameters are gathered through simulation, and flight risk is calculated using EVT [13].

6) Combining the results of Step 3 and Step 5, safety verification and measures for improving flight safety are obtained, which is the goal of this method.

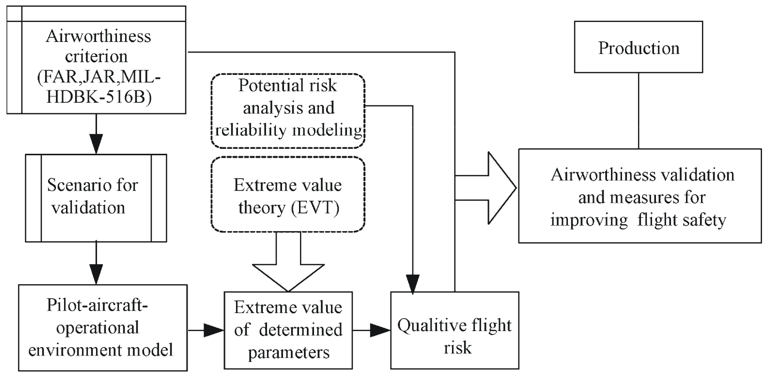

Fig.12 Airworthiness compliance verification process based on complex system simulation.

6. Exemplification

The failure in fly-by-wire system may cause catastrophic consequence. How to improve its safety and reliability is a key technology in its development. The reliability of fly-by-wire system is critical to flight safety. So the Clause 6.2.4.2 in VCFs in Chapter 6 of MIL-HDBK-516B is selected to be verified.

6.1. *Analysis of airworthiness clause and scenario foundation*

The Clause 6.2.4.2 regulates that flight risk caused by single point failures of VCFs should be "acceptable". The quantitative requirement of fly-by-wire system is regulated by GJB2878-97 "general specification for fly-by-wire flight control system of piloted aircraft (fixed wing)" from three aspects including catastrophic failure, loss probability of aircraft and availability of urgent/spare system. The loss probability caused by failure of flight control system is prescribed quantitatively in GJB2878-97. Flight accident risk of light aircraft and fighter is no more than 100×10^{-7}/h [16]. The assessment probability is verified according to this quantitative standard in the following part. Measures and index suggestion for aircraft design can be obtained by verification [17].

6.2. Complex modeling and simulation

Flight testing scenario of this clause is founded in Section 2.1, and is shown in Fig. 1. Modeling and simulation are based on this scenario.

Firstly, the failure model of the scenario is founded. The failure of overload sensor in fly-by-wire system can cause uncommanded deflection of elevator, and the deflection step of elevator can cause a sudden elevation or descent, which may lead to the paranormal of n_z and α. A negative elevator angle can cause nondirective elevation, and the angle of attack is selected as a crucial parameter. A positive elevator angle may cause nondirective decent, and overload is the crucial parameter.

The failure model of overload sensor is stuck model $y_{i\text{out}}(t)=a_i$. It is analyzed statistically that the failure value of elevator deflection conforms to the normal distribution with maximum and minimum values [5]; the region of value is (−8°, 8°).

The failure value of roll rate sensor conforms to uniform distribution. The mathematical expression of failure model is

$$x_i=\begin{cases}x_{it} & \text{Normal}\\ x_{\min}+(x_{\max}-x_{\min})\times \text{Rand}(0,1) & \text{Failure}\end{cases} \tag{17}$$

where x_i is the value of sensor, x_{it} the normal operating value of roll rate sensor, and Rand (0,1) a random number in the region of (0,1). The failure value of aileron deflection is (−5°,3°). Histogram of failure angle of elevator or aileron is established, as shown in Fig. 13.

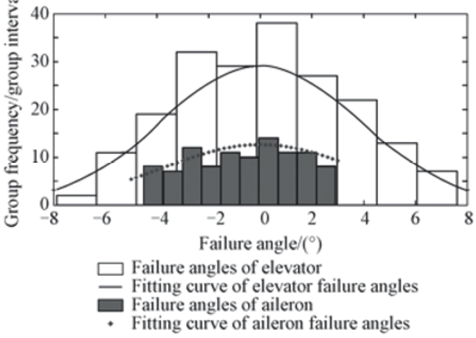

Fig. 13 Deflection of elevator and aileron caused by two sensors.

The non-linear six-degree-of-freedom mathematical model of aircraft flight dynamics is programmed in MATLAB 7.4. pilot manipulation model in critical situation which is illuminated in Section 2.2, is chosen as the pilot model in this example.

After the establishment of pilot, aircraft and failure models, a virtual flight testing method based on the connection of MATLAB/Simulink and Flightgear is proposed. The simulation framework of the method is shown in Fig. 14.

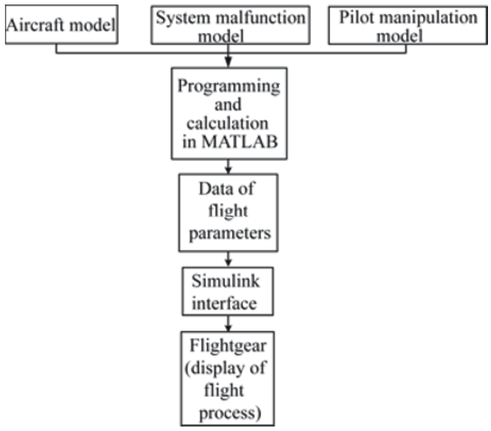

Fig. 14 Simulation framework based on connection of MATLAB/Simulink and Flightgear.

Failure deflection and pilot manipulation are the inputs of the simulation, and the outputs are AOA, n_z and p, etc. Flight after two sensors' malfunction is simulated, and part of simulation results is shown in Figs. 15-17.

Fig. 15 Pilot's visual in the beginning of simulation.

Fig. 16 Rapid pitching of aircraft caused by n_z sensor's failure.

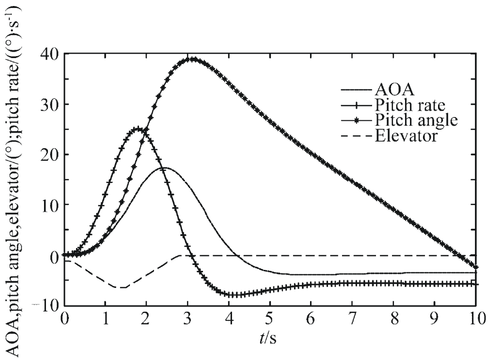

Fig. 17 AOA, pitch angle, pitch rate and elevator variation with time after failure of n_z sensor.

6.3. *Calculation of flight risk as caused by single failure*

The complex system is simulated with the Monte-Carlo method. And extremum samples of α, n_z or p can be obtained.

1) Flight risk probability caused by overload sensor

Repeat the simulation with Monte-Carlo for 100 times, and 100 values of elevator angle were obtained; 57 values are negative, and the others are positive.

Risk probability calculated by the small probability assessment method based on EVT (nonlinear regress model) is 0.033 6, which evaluates negative failure deflection. The relationship between extreme value and standard warp is shown in Fig. 18.

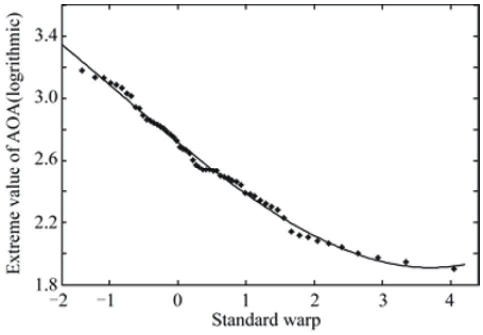

Fig. 18 Sample extreme value and standard warp (AOA).

Similarly, the extreme values of n_z are used to calculate the flight risk based on EVT (linear regress model). The result is 0.036 6. The relationship between the extreme value and standard warp is shown in Fig. 19.

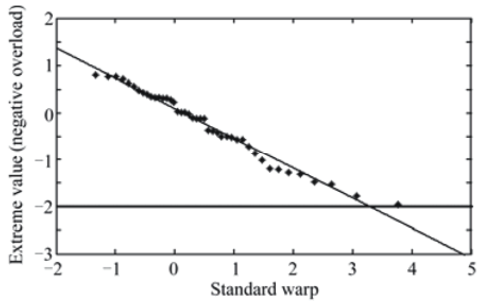

Fig. 19 Sample extreme value and standard warp (negative overload).

The failure probability of this overload sensor conforms to Weibull distribution according to the conclusion in Section 3. In this case, it has been used for 100 h, so the failure rate is $\lambda(100) = 2.0\times10^{-5}$. So the flight risk probability caused by this overload sensor is

$$Q = P\lambda = 1.4\times10^{-6} \tag{18}$$

It is shown that aircraft loss probability in one hour caused by the failure of this system satisfies the quantitative requirement of GJB2878-97. Thus, it cannot satisfy the requirement of MIL-HDBK-516B.

2) Risk probability caused by roll rate sensor

The largest permitted value of roll rate is 90°/s. Similarly, risk probability obtained from the small probability assessment method based on EVT is 0.054 5.

The reliability of roll rate sensor in landscape orientation channel submits to exponential distribution, and the failure probability is 3.0×10^{-4}. The total risk of each flight in one hour is

$$Q = 3.0\times10^{-4}\times5.45\times10^{-2} = 1.64\times10^{-5} \tag{19}$$

It means that the flight risk caused by this failure does not satisfy the quantitative demand of GJB2878-97.

In summary, this flight control system cannot satisfy the requirement of the Clause 6.2.4.2 in MIL-HDBK-516B. Thus, corresponding flight safety measures must be taken to improve it. The flight risk caused by equipment failure is closely related to the reliability of components and the interaction between components. Therefore, three pieces of advice are brought forward. First, the reliability of this n_z sensor should be improved, or it should be changed to a new one at earlier time. Second, the influence of failure must be weakened, so as to improve the robustness of the pilot-aircraft system. Third, pilot training of such kind of situation should be emphasized.

7. Conclusions

A method has been developed for airworthiness compliance verification based on pilot-aircraft-environment complex system simulation. Special researches are conducted on verification scenarios, stochastic pilot modeling, optimized risk evaluation model and virtual flight testing. The method is fit for both civilian and military aircraft.

The distinguishing advantages of this method include its low cost, good repeatability and controllability in airworthiness verification research. The proposed method can also focus on complex and high-risk situations difficult to research by real flight testing. Thus, more valuable conclusions can be obtained for airworthiness verification and aircraft safety design.

The challenge of future work may include modeling and simulation of aircraft safety critical systems and their dynamic performance analysis after failure. Meanwhile, validation of simulation results is another challenge.

References

[1] Scharl J, Mavris D N, Burdun I Y. Use of flight simulation in early design: formulation and application of the virtual testing and evaluation methodology. AIAA-2000-5590, 2000.

[2] Crum V, Homan D, Bortner R. Certification challenges for autonomous flight control systems. AIAA Guidance, Navigation, and Control Conference and Exhibit, 2007; 2097-3001.

[3] Belcastro C M. On the validation of safety critical aircraft systems, part I: analytical & simulation methods. AIAA-2003-5560, 2003.

[4] Baltes E, Spitz W. Virtual flight test as advanced step in aircraft development. AIAA-2002-5823, 2002.

[5] Иванов В С, Воробьёв В В. Безопасность полетов летательных аппаратов. Москва: ВВИА, 2003. [in Russian]

[6] Dreger H, Bremers E. Airworthiness verification of an airborne telescope in practice. Proceeding of SPIE, 2003; 321-332.

[7] ARP4761. Aerospace recommended practice: guidelines and methods for conducting the safety assessment process on civil airborne systems and equipment. U.S. SAE, 1996.

[8] MIL-HDBK-516B. Airworthiness certification criteria. New York: U.S. Department of Defense Handbook, 2004.

[9] Ge P H. Safety aviation of airplane. Beijing: Press of Safety Aviation Institute of Air Force, 2004. [in Chinese]

[10] Бюшгенс Г С. Аэродинамика, устойчивость иуправ ляемость сверхзвуковых самолетов. Москва: НАУКА ФИЗМАТЛИТ, 1998. [in Russian]

[11] Huang C T, Wang L X. Effects of rain and wind on aircraft flight safety. Acta Aeronautica et Astronautica Sinica 2010; 31(4): 694-700. [in Chinese]

[12] Gérard O. Maximum field inside a reverberation chamber modeled by the generalized extreme value distribution. IEEE Transactions on Electromagnetic Compatibility 2007; 49(1): 104-113.

[13] Davisa R A, Mikoschb T. Extreme value theory for space-time processes with heavy-tailed distributions. Stochastic Processes and their Applications 2008; 118(4): 560-584.

[14] Bayley D J. Design optimization of a space launch vehicle using a genetic algorithm. Journal of Spacecraft and Rockets 2008; 45(4): 733-740.

[15] Thierens D, Goldberg D. Elitist recombination: an integrated selection recombination GA. The First IEEE Conference on Evolutionary Computation, Orlando, Floride, 1994; 263-269.

[16] Department of Aeronautics Industry. GJB2878-97. General specification for fly-by-wire flight control system of piloted aircraft(fixed wing). Beijing: Technology and Industry for National Defense, 1997. [in Chinese]

[17] Zoughbi G, Briand L, Labiche Y. A UML profile for developing airworthiness-compliant (RTCA DO-178B) safety-critical software. Berlin Heidelberg: Springer-Verlag, 2007; 574-588.

Biographies:

XU Haojun is a professor in Air Force Engineering University. His area of research covers flight safety and combat effectiveness evaluation.
E-mail: xuhaojun@mail.xjtu.edu.cn

LIU Dongliang received B.S and M.S. degrees from Air Force Engineering University. His main research interests lie in flight safety and complex system simulation.
E-mail: oxygenldl09@163.com